Author Manuscript

Author Manuscript

Author Manuscript

Author Manuscript

HHS Public Access

Author manuscript

Nature. Author manuscript; available in PMC 2014 June 12.

Published in final edited form as:

Nature. 2013 December 12; 504(7479): 254–259. doi:10.1038/nature12725.

Structural mechanism of ligand activation in human $GABA_B$ receptor

Yong Geng[1], **Martin Bush**[1], **Lidia Mosyak**[1], **Feng Wang**[1], and **Qing R. Fan**[1,2]

[1]Department of Pharmacology, Columbia University, New York, NY, USA

[2]Department of Pathology & Cell Biology, Columbia University, New York, NY, USA

Abstract

Human $GABA_B$ receptor is a G-protein coupled receptor central to inhibitory neurotransmission in the brain. It functions as an obligatory heterodimer of GBR1 and GBR2 subunits. Here we present the first crystal structures of a heterodimeric complex between the extracellular domains of GBR1 and GBR2 in the apo, agonist-bound, and antagonist-bound forms. The apo and antagonist-bound structures represent the resting state of the receptor; the agonist-bound complex corresponds to the active state. Both subunits adopt an open conformation at rest, and only GBR1 closes upon agonist-induced receptor activation. The agonists and antagonists are anchored in the interdomain crevice of GBR1 by an overlapping set of residues. An antagonist confines GBR1 to the open conformation of the inactive state, while an agonist induces its domain closure for activation. Our data reveals a unique activation mechanism for $GABA_B$ receptor that involves the formation of a novel heterodimer interface between subunits.

GABA (γ-amino butyric acid) is the predominant inhibitory neurotransmitter in the central nervous system. Metabotropic $GABA_B$ receptor is a G-protein coupled receptor (GPCR) that mediates slow and prolonged synaptic inhibition through $G_{i/o}$ protein[1,2]. Presynaptic $GABA_B$ receptor suppresses neurotransmitter release, and postsynaptic $GABA_B$ receptor causes hyperpolarization of neurons[1,2]. Malfunction of $GABA_B$ receptor can lead to various neurological disorders, including spasticity, epilepsy, and pain[1–3]. Baclofen, a selective $GABA_B$ agonist, is used clinically to treat muscle spasticity associated with multiple sclerosis, cerebral palsy, and spinal cord injury[1–3].

Users may view, print, copy, download and text and data- mine the content in such documents, for the purposes of academic research, subject always to the full Conditions of use: http://www.nature.com/authors/editorial_policies/license.html#terms

Correspondence and request for materials should be addressed to Q.R.F. (qf13@columbia.edu).

Supplementary Information is linked to the online version of the paper at www.nature/com/nature.

Author contributions

Q.R.F. conceived the study and designed the experiments; Y.G., Q.R.F., M.B., L.M. and F.W. performed experiments and analyzed data, Q.R.F. and Y.G. wrote the paper.

Author information

Atomic coordinates and diffraction data are deposited in the RCSB PDB with accession codes 4MQE, 4MQF, 4MR7, 4MR8, 4MR9, 4MRM, 4MS1, 4MS3, and 4MS4.

The authors declare no competing financial interests.

Author Manuscript Author Manuscript Author Manuscript Author Manuscript

$GABA_B$ receptor belongs to the distinct class C GPCR family[4]. Ligand-binding to these receptors takes place within a large extracellular Venus Flytrap (VFT) module that has sequence homology to bacterial periplasmic amino acid binding proteins (PBPs)[4]. Unlike metabotropic glutamate receptors (mGluRs) and extracellular calcium sensing receptor, which function as disulfide-tethered homodimers[5–8], $GABA_B$ and taste receptors act as heterodimers[9–16].

$GABA_B$ receptor functions as a heterodimeric assembly of GBR1 and GBR2 subunits[9–12,14]. GBR2 facilitates cell surface expression of GBR1 by masking an endoplasmic reticulum retention signal of GBR1[17,18]. GBR1 is responsible for ligand recognition through its extracellular domain[19,20]. Although GBR2 does not bind any known $GABA_B$ ligand[9–11,21], its ectodomain directly interacts with the GBR1 ectodomain to enhance agonist affinity[10,11,22–26] and is required for receptor activation[22,25,27]. Finally, the transmembrane domain of GBR2 is responsible for G-protein coupling[22,25,28–32].

Most of the current knowledge about class C GPCR structures derives from homodimeric mGluRs. The ectodomain structures of three mGluR subtypes have been determined with and without ligand[33–35]. Here we assembled a stable heterodimeric complex of the human GBR1 and GBR2 ectodomains, and determined its crystal structure in the absence of ligand and in the presence of various agonists and antagonists. Together with our mutational data, these structures provide insights into the molecular mechanisms of receptor heterodimerization, ligand recognition, and receptor activation.

Structures of $GABA_B$ heterodimer

The extracellular VFT module of human GBR1b ($GBR1b_{VFT}$) and GBR2 ($GBR2_{VFT}$) were co-secreted as a heterodimeric complex from insect cells (Supplementary Fig. 1). The $GBR1b_{VFT}$:$GBR2_{VFT}$ heterodimer binds various agonists and antagonists with the same rank order of affinities as the full-length receptor, indicating that it is physiologically relevant[26].

We determined the crystal structure of the $GBR1b_{VFT}$:$GBR2_{VFT}$ complex in the apo form, bound to six different antagonists ($CGP54626_{ANT}$, $CGP46381_{ANT}$, $CGP35348_{ANT}$, $SCH50911_{ANT}$, (S)-2-OH-$saclofen_{ANT}$, and (R)-$phaclofen_{ANT}$), and bound to two different agonists (endogenous ligand GABA and clinical drug (R)-$baclofen_{AGO}$) (Supplementary Table 1). Each structure consists of a non-covalent heterodimer of $GBR1b_{VFT}$ and $GBR2_{VFT}$, wherein the two subunits “dance cheek-to-cheek”: the protomers are bound to each other such that they are side by side and facing opposite directions (Fig. 1a–c; Supplementary Fig. 2). All of the agonists and antagonists bind in the crevice between the LB1 and LB2 domains of $GBR1b_{VFT}$.

$GBR1b_{VFT}$ and $GBR2_{VFT}$ have similar overall structures, in agreement with their sequence homology (33% identity) (Supplementary Fig. 3). Both subunits have a bi-lobed architecture related to that found in mGluRs[33–35], natriuretic peptide receptors[36,37], ionotropic glutamate receptors[38–40] and PBPs[41]. However, the extracellular domains of GBR1b and GBR2 lack the cysteine-rich region found at the C-terminal end of mGluR ectodomains. Each $GABA_B$

Author Manuscript Author Manuscript Author Manuscript Author Manuscript

subunit contains two distinct domains, LB1 and LB2. The individual LB1 and LB2 domains of the two subunits exhibit high correlation with each other.

Despite similarities, the $GBR1b_{VFT}$ and $GBR2_{VFT}$ structures have different interdomain arrangements, consistent with their disparate ligand-binding characteristics (Fig. 2a, b). The ligand-binding subunit $GBR1b_{VFT}$ can oscillate between open and closed conformations, wherein the more compact closed conformation is associated with agonist binding. In contrast, the non-ligand binding subunit $GBR2_{VFT}$ has nearly identical conformations with and without dimer partner $GBR1_{VFT}$.

In the crystal structure of apo-$GBR1b_{VFT}$:$GBR2_{VFT}$, both subunits adopt an open conformation when compared with the known structures of mGluRs[33–35] (Supplementary Fig. 4). All six antagonist-bound structures closely resemble that of the apo complex, both in the arrangement of the heterodimer and in the structures of the individual subunits (Supplementary Fig. 4). The ligand-binding cleft of $GBR1b_{VFT}$ stays open with each bound antagonist. In addition, $GBR2_{VFT}$ remains wide open with an empty interdomain cleft. This open-open configuration of the apo and antagonist-bound structures corresponds to the resting (or inactive) state of the heterodimeric receptor.

Agonist binding causes large conformational changes within the heterodimeric complex. First, both the agonists GABA and (R)-$baclofen_{AGO}$ induce domain closure of $GBR1b_{VFT}$, as previously predicted[42] (Fig. 2a). When the LB1 domains of apo and agonist-bound $GBR1b_{VFT}$ are superimposed, their LB2 domains can be related by a 29°-rotation about a nearly horizontal interdomain axis. Since the rotational axis has a slight vertical offset, this transformation also brings the LB2 domain of $GBR1b_{VFT}$ into close contact with the LB2 domain of $GBR2_{VFT}$ to form a large heterodimer interface unique to the active state.

Second, $GBR2_{VFT}$ remains open in the agonist-bound state, consistent with our previous prediction that $GBR2_{VFT}$ has a constitutively open conformation[26]. Nevertheless, the LB2 domain of $GBR2_{VFT}$ undergoes a twist motion of 9° around a nearly vertical axis, and moves toward the LB2 domain of $GBR1b_{VFT}$ to form new heterodimeric contacts (Fig. 2b).

Finally, the substantial rearrangement of the LB2 domains from the apo to the agonist-bound state shortens the distance between the C-termini of the two subunits from 45 Å to 32 Å (Fig. 2c, d; Supplementary Fig. 5). This decrease in the separation between membrane proximal LB2 domains may lead to changes in the relative orientation of the transmembrane domains. In summary, both agonist-bound $GBR1b_{VFT}$:$GBR2_{VFT}$ complexes adopt a closed-open structural arrangement, which corresponds to the active state of the receptor (Supplementary Fig. 4).

Common subunit-subunit interactions

In both the resting and active states, $GBR1b_{VFT}$ and $GBR2_{VFT}$ interact through their LB1 domains (Supplementary Fig. 6, 7). In the apo and antagonist-bound structures, the subunit association is exclusively facilitated by this LB1-LB1 contact. The heterodimer buries over 1,400 $Å^2$ of solvent accessible surface area and exhibits exceptionally high interfacial shape correlation (Supplementary Table 2).

Author Manuscript Author Manuscript Author Manuscript Author Manuscript

The LB1-LB1 interaction is mediated by the B and C helices of both subunits (Fig. 3a). The heterodimer interface can be divided into three regions (Fig. 3b). Site I is located at the center of the interface, and it is flanked by sites II and III on each side.

Site I is comprised of a central hydrophobic patch surrounded by hydrogen bonds. The heterodimer contacts within this site are highly conserved in all of the $GBR1b_{VFT}$:$GBR2_{VFT}$ structures. In particular, it features three deeply buried tyrosine residues (Y113 and Y117 of $GBR1b_{VFT}$, and Y118 of $GBR2_{VFT}$) that are critical for heterodimer interaction and receptor activation[26]. These tyrosine residues participate in aromatic stacking interactions, and form interfacial hydrogen bonds. Together with the adjacent lysine and tryptophan residues, they are responsible for the majority of hydrophobic contacts at the LB1-LB1 heterodimer interface.

Site II interactions are mostly hydrogen bonds, and include a universal salt bridge ($GBR1b_{VFT}$-R141 : $GBR2_{VFT}$-D109) as well as a conserved hydrogen bond ($GBR1b_{VFT}$-E138 : $GBR2_{VFT}$-N110). Site III consists predominantly of water-mediated contacts, and is the most variable part of the LB1-LB1 interface.

Agonist-induced heterodimer interface

Agonist binding induces the formation of an additional heterodimer interface between the LB2 domains of $GBR1b_{VFT}$ and $GBR2_{VFT}$ subunits (Supplementary Fig. 7). This is consistent with our calorimetry measurements showing that $GBR2_{VFT}$ has higher affinity for agonist-bound than antagonist-bound $GBR1b_{VFT}$[26]. The LB2-LB2 interface buries over 1,300 $Å^2$ of solvent accessible surface area, has poor shape complementarity, and is dominated by polar interactions (Supplementary Table 2).

The LB2-LB2 interaction is mediated by two strand-loop-helix motifs from each LB2 domain (Fig. 3c). The neighboring strands f and g are part of the central β-sheet in LB2, and helices F and G flank the β-sheet. The heterodimer contacts consist primarily of hydrogen bonds, some of which are mediated by water molecules. The interface can be divided into three adjacent areas (Fig. 3d). Sites IV and V each feature a large cluster of hydrogen bonds, while site VI mostly consists of isolated contacts. The $GBR2_{VFT}$ residue N213 is located at the intersection of sites IV and V, and it bridges the hydrogen bond networks within these two regions. In addition, a minor LB2-LB1 contact involving helix D of $GBR2_{VFT}$ is formed at the edge of site IV.

To confirm the importance of the LB2-LB2 heterodimer interface to receptor activation, we carried out alanine scanning mutagenesis of the interfacial residues. We identified several polar residues from each subunit that are critical to agonist-dependent G_i protein activity (Supplementary Fig. 7). These include the $GBR1b_{VFT}$ residues T198, E201 and S225, and the $GBR2_{VFT}$ residues D204, Q206, N213 and S233. All of these residues are engaged in multiple interfacial hydrogen bonds at the LB2-LB2 interface. This reliance on hydrophilic interactions to form a distinct subunit interface in the active state allows the receptor to readily dissociate upon returning to its resting state. Previous studies have also shown that introduction of a large N-glycan into the LB2 domain of either $GABA_B$ subunit inhibits agonist-induced receptor activation[43].

Author Manuscript Author Manuscript Author Manuscript Author Manuscript

Ligand recognition

All of the antagonists are derivatives of GABA, and have the general structure of a γ-amino acid. The receptor-antagonist interactions are mediated largely by hydrogen bonds (Fig. 4a, b; Supplementary Fig. 8). First, each antagonist is anchored at the crevice of $GBR1b_{VFT}$ by two sets of hydrogen bonds. The α-acid group at one end forms hydrogen bonds with the LB1 residues S130 and S153; the γ-amino group at the other end is hydrogen-bonded to H170 and E349. Second, W65 makes van der Waals contacts with all of the antagonists. Third, the β-hydroxyl substituent of $CGP54626_{ANT}$ and (S)-2-OH-saclofen makes additional hydrogen bonds with the receptor that are specific to these antagonists. Finally, all of the antagonists except $SCH50911_{ANT}$ and (R)-$phaclofen_{ANT}$ participate in water-mediated interaction with S131. These extensive contacts indicate that the LB1 domain is primarily responsible for anchoring antagonist.

In contrast, the interaction between the LB2 domain and bound antagonist is sparse and varies among the different antagonists (Supplementary Fig. 8). Only two antagonists, $CGP54626_{ANT}$ and $SCH50911_{ANT}$, directly contact W278 of LB2 through a large γ-substituent. As a result of this additional LB2 interaction, both compounds have higher binding affinity to $GABA_B$ receptor than the other antagonists reported here[3]. This suggests that the LB2 domain plays an auxiliary role in antagonist recognition, and enhances the potency of selective antagonists.

$GABA_B$ receptor recognizes both the agonists GABA and (R)-$baclofen_{AGO}$ in essentially the same manner (Fig. 4c, d; Supplementary Fig. 9). (R)-$baclofen_{AGO}$ is a derivative of GABA, and contains a chlorophenyl substituent at the β-position. Like the antagonists, each agonist is secured by two hydrogen bond networks, one at each end of the molecule. Furthermore, a common set of LB1 residues are involved in binding the two ends of all of the agonists and antagonists. Unlike the antagonists, both agonists also directly contact two key residues of the LB2 domain, Y250 and W278. In addition, the two tryptophan residues W65 and W278 make extensive van der Waals contacts with both GABA and (R)-$baclofen_{AGO}$. Therefore, both the LB1 and LB2 domains are required for agonist recognition.

The binding sites of GABA and (R)-$baclofen_{AGO}$ differ in the side chain conformation of the LB2 residue W278 (Supplementary Fig. 9). Relative to its orientation in the GABA-bound complex, the indole ring of W278 is flipped ~170° to accommodate the β-chlorophenyl substituent of (R)-$baclofen_{AGO}$, which forms aromatic ring-stacking interactions with both Y250 and W278. In contrast, GABA makes van der Waals contact with W278 alone through its aliphatic backbone. The conformational adaptability of W278 provides a mechanism by which the receptor recognizes structurally different ligands while maintaining ligand-binding specificity and affinity.

Agonist versus antagonist action

The function of a $GABA_B$ agonist is to stabilize the closed conformation of $GBR1b_{VFT}$, while that of an antagonist is to confine the $GBR1b_{VFT}$ subunit to the open configuration (Supplementary Fig. 10). Agonist-bound $GBR1b_{VFT}$ has a closed cleft; the agonist is buried

Author Manuscript Author Manuscript Author Manuscript Author Manuscript

and inaccessible to the bulk solvent. In contrast, antagonist-bound $GBR1b_{VFT}$ has an open cleft, and the antagonist is solvent accessible.

The presence of a bulky substituent in each antagonist inhibits domain closure of $GBR1b_{VFT}$. The highly potent antagonist $CGP54626_{ANT}$ contains an α-cyclohexyl and a γ-dichlorophenyl group. The adverse interactions of these moieties with Y250 and W278 would be expected to prevent the LB1 and LB2 domains from approaching each other (Fig. 4e). Similarly, each of the other antagonists $CGP46381_{ANT}$, $CGP35348_{ANT}$, and $SCH50911_{ANT}$ has a bulky substituent at either the α- or γ-position to block $GBR1b_{VFT}$ domain closure (Supplementary Fig. 8, 9). Although the antagonists (S)-2-OH-$saclofen_{ANT}$ and (R)-$phaclofen_{ANT}$ are structurally analogous to the agonist (R)-$baclofen_{AGO}$, their α-acid motifs assume a tetrahedral coordination geometry that is incompatible with the active-state conformation of Y250 (Fig. 4f). Furthermore, the α-substituents push the β-chlorophenyl ring toward the γ-amino end of each antagonist, thereby generating potential steric interactions with I276 and W278 to prevent $GBR1b_{VFT}$ domain closure.

All of the residues at the ligand-binding site are conserved within GBR1 sequences across different species (Supplementary Fig. 11). Some of the ligand-binding residues have been implicated by previous studies, including S130, G151, S153 and E349 of GBR1b[21,26,44–46].

The LB1 residues are required for both agonist and antagonist recognition. We found that the W65A substitution caused substantial loss of ligand binding and receptor function, (Fig. 4g, h). The H170A mutation essentially abolished antagonist binding, and lowered the maximum agonist-induced [^{35}S]GTPγS binding to half that of wild-type level (Fig. 4g, h). These data indicate that both W65 and H170 are indispensable for ligand recognition.

The LB2 residues are essential for agonist binding. First, the W278A mutant retained the ability to bind the antagonist [^{3}H]$CGP54626_{ANT}$, although with decreased potency (Fig. 4g). This is consistent with the auxiliary role of W278 in antagonist recognition. On the other hand, this mutation is detrimental to receptor activation, since it not only reduced the maximum GABA-dependent [^{35}S]GTPγS binding, but also increased the half effective concentration (EC_{50}) of GABA by more than 500-fold (Fig. 4h). Second, the Y250A mutation had no effect on antagonist binding, in agreement with our structural observations (Fig. 4g). However, it decreased the agonist response, and increased the EC_{50} of GABA by more than 100-fold (Fig. 4h). These data indicate that both Y250 and W278 are critical to agonist recognition.

Implications for receptor activation

Structural comparison indicates that the concept of major inter-subunit relocation that holds for the activation of mGluRs cannot be applied to $GABA_B$ receptor. The extracellular domains of these receptors share a common mode of dimerization through their LB1 domains (Supplementary Fig. 12, 13). The resting and active configurations of mGluRs differ by a 70°-rotation in dimer orientation[33–35]. Both closed-open and closed-closed conformations have been reported for activated mGluRs[33–35], although full activation requires the closure of both protomers[47]. In contrast, the heterodimeric LB1-LB1 interface of $GABA_B$ receptor undergoes a minor 5°-rearrangement upon agonist binding, and the

Author Manuscript Author Manuscript Author Manuscript Author Manuscript

receptor only adopts a closed-open active conformation. Our data indicate that activation of $GABA_B$ receptor involves the formation of a novel LB2-LB2 heterodimer interface.

We carried out disulfide crosslinking studies[48] to determine the physiological relevance of the LB2-LB2 interaction in full length receptor. Based on the active-state structure of $GBR1b_{VFT}$:$GBR2_{VFT}$, we introduced cysteine mutations into a residue pair across the LB2-LB2 dimer interface (GBR1-T198C and GBR2-Q206C), which had the proximity and geometry required for disulfide formation (Fig. 5a). Western blot analysis indicates that co-expression of wild-type GBR1b and GBR2 or the combination of a single cysteine mutant with its wild-type partner in mammalian cells produced monomeric protein bands in the presence of GABA under both reducing and non-reducing conditions (~95 kDa for GBR1b; ~115 kDa for GBR2) (Fig. 5b). In contrast, co-expression of the cysteine mutant pair yielded a heterodimeric protein band (~210 kDa) under non-reducing conditions (Fig. 5b). This band was recognized by both anti-Flag and anti-HA antibodies, which were used to detect differentially tagged GBR1b and GBR2 subunits. Furthermore, it was observed in the absence of ligand and in the presence of the agonist GABA. These observations indicate the spontaneous formation of a disulfide-tethered GBR1b-GBR2 heterodimer, and confirm that the LB2-LB2 interface observed in the active-state $GBR1b_{VFT}$:$GBR2_{VFT}$ structure is also present in free and agonist-bound native $GABA_B$ receptor.

To determine the functional effects of locking the LB2-LB2 interface, we measured agonist-dependent G_i protein activation of different combinations of wild-type and cysteine mutant receptors (Fig. 5c). For the wild-type receptor and single cysteine mutants, application of GABA led to stimulation of [^{35}S]GTPγS binding both in the absence and presence of dithiothreitol (DTT). In contrast, the double cysteine mutant exhibited constitutive activity under non-reducing conditions, and addition of GABA did not further increase its functional activity (Fig. 5c). This indicates that the inter-subunit disulfide bond holds the receptor in a fully active form. Indeed, upon reduction of the disulfide bond, the double cysteine mutant receptor lost its constitutive activity, but regained sensitivity to GABA to a level comparable to that of a single cysteine mutant (Fig. 5c). Our data demonstrate that formation of the LB2-LB2 interface is both necessary and sufficient for $GABA_B$ receptor activation.

In the conformational equilibrium of $GABA_B$ receptor, an antagonist maintains the inactive conformation of the receptor, while an agonist stabilizes its active conformation (Supplementary Fig. 14). Agonist binding to $GABA_B$ receptor induces domain closure in the GBR1 subunit, an expansion of the heterodimer interaction to include a large LB2-LB2 interface, and a decrease in the separation between the membrane-proximal LB2 domains. Since receptor function is not affected by alterations in the peptide linker between the VFT and transmembrane domains of each subunit[27], these changes would likely be directly relayed to the transmembrane domains. We expect that the transmembrane domains of the $GABA_B$ subunits exist as pre-formed heterodimers on the cell surface because both the extracellular and intracellular components form stable heterodimers[12,23,24,26,49]. Therefore, agonist-induced conformational changes may lead to a rearrangement of the transmembrane domain heterodimer for signal transduction across the membrane. This novel activation mechanism would be, as of yet, unique to inhibitory $GABA_B$ receptor.

Author Manuscript Author Manuscript Author Manuscript Author Manuscript

Methods

Protein expression and purification

The extracellular domains of human GBR1 and GBR2 were separately cloned into the pFBDM vector[50] for expression in baculovirus-infected insect cells. The GBR1 isoform GBR1b[19] was used in this study. The $GBR1b_{VFT}$ construct contained residues 48–459, with the signal peptide of baculovirus envelope surface glycoprotein gp67 attached at the N-terminus and a Flag tag at the C-terminus. The $GBR2_{VFT}$ construct contained residues 1–466 and a C-terminal Flag tag, as previously described[26].

Sf9 insect cells were co-infected with recombinant $GBR1b_{VFT}$ and $GBR2_{VFT}$ baculoviruses at 23°C for 96 hours. The $GBR1b_{VFT}$:$GBR2_{VFT}$ complex was purified from cell supernatant by anti-Flag antibody (M2) affinity chromatography followed by gel filtration chromatography (Superdex 200, GE Healthcare). The $CGP54626_{ANT}$-$GBR1b_{VFT}$:$GBR2_{VFT}$ complex was produced in the presence of 10 μM $CGP54626_{ANT}$ throughout expression and 20 μM $CGP54626_{ANT}$ during purification. The (R)-$baclofen_{AGO}$-$GBR1b_{VFT}$:$GBR2_{VFT}$ complex was expressed and purified in the presence of 100 μM (R)-baclofen, and the GABA-$GBR1b_{VFT}$:$GBR2_{VFT}$ complex was produced in the presence of 100 μM GABA.

Crystallization and data collection

Crystals of the apo-$GBR1b_{VFT}$:$GBR2_{VFT}$ complex were grown at 4°C in 10% PEG 3350, 20% glycerol and 0.12 M Na acetate, pH 7.0. Crystals of various antagonist-bound $GBR1b_{VFT}$:$GBR2_{VFT}$ complexes were obtained under the same condition as the apo complex. Specifically, the $CGP54626_{ANT}$-bound heterodimer was crystallized using protein that was purified in the presence of $CGP54626_{ANT}$. The apo-$GBR1b_{VFT}$:$GBR2_{VFT}$ complex was also co-crystallized with 10 mM of each of the following antagonists: $CGP46381_{ANT}$, $CGP35348_{ANT}$, $SCH50911_{ANT}$, (R, S)-2-OH-$saclofen_{ANT}$, and (R, S)-$phaclofen_{ANT}$. All of the crystals were directly frozen from drops.

The agonist-bound (R)-$baclofen_{AGO}$-$GBR1b_{VFT}$:$GBR2_{VFT}$ complex was crystallized at 20°C from 20% PEG 2000, 15% glycerol, 0.2 M NH_4Cl, and 0.1 M Na cacodylate, pH 5.2, in the presence of 10 mM (R)-baclofen. Crystals of the GABA-$GBR1b_{VFT}$:$GBR2_{VFT}$ complex were grown at 20°C from 18% PEG 2000, 5% glycerol, 0.15 M NH_4Cl, and 0.1 M Na cacodylate, pH 5.0, in the presence of 10 mM GABA. The crystals were frozen in a cryoprotecting solution containing 20% glycerol and all other components of the crystallization solution.

Native data for the different complexes were collected at the 24ID-C and 24ID-E beamlines of Advanced Photon Source (APS). Diffraction data for the apo, $CGP46381_{ANT}$-, $CGP35348_{ANT}$-, $SCH50911_{ANT}$-, and GABA-bound complexes were integrated using XDS[51] and scaled with SCALA[52]. Data for the $CGP54626_{ANT}$-, (S)-2-OH-$saclofen_{ANT}$-, (R)-$phaclofen_{ANT}$-, and (R)-$baclofen_{AGO}$-bound complexes were integrated and scaled using HKL2000[53].

Author Manuscript Author Manuscript Author Manuscript Author Manuscript

Structure determination

The structure of the apo-GBR1b$_{VFT}$:GBR2$_{VFT}$ complex was solved by molecular replacement. The position of GBR2$_{VFT}$ was identified using the free GBR2$_{VFT}$ structure (PDB code 4F11)[26] as the search model. The location of GBR1b$_{VFT}$ was found using the individual LB1 and LB2 domains of GBR2$_{VFT}$ as the search probes. A complete atomic model of the apo-GBR1b$_{VFT}$:GBR2$_{VFT}$ complex was developed through a succession of manual building and iterative refinement. The final model contained the GBR1b$_{VFT}$ residues 48–368 and 377–459, the GBR2$_{VFT}$ residues 53–292, 300–379 and 385–466, and part of the Flag tag at the C-termini of both subunits. Carbohydrate residues were also attached to Asn323 and Asn365 of GBR1b$_{VFT}$, and Asn404 of GBR2$_{VFT}$.

All of the antagonist-bound GBR1b$_{VFT}$:GBR2$_{VFT}$ structures were solved by molecular replacement using the apo-GBR1b$_{VFT}$:GBR2$_{VFT}$ structure as the search model. For each complex, the bound antagonist was modeled into the residual electron density map obtained in the final rounds of refinement. All of the antagonist-bound structures contained the GBR1b$_{VFT}$ residues 48–368 and 377–459, the GBR2$_{VFT}$ residues 53–292, 300–379 and 385–466, and part of the Flag tag at the C-termini of both subunits. Carbohydrate residues were also attached to Asn323 and Asn365 of GBR1b$_{VFT}$, and Asn404 of GBR2$_{VFT}$. Although a racemic mixture (R, S)-2-OH-saclofen$_{ANT}$ was used for crystallization, only the (S)-2-OH-saclofen$_{ANT}$ enantiomer was bound to GBR1b$_{VFT}$ in the structure. Our observation is consistent with previous findings that (S)-2-OH-saclofen$_{ANT}$ enantiomer is the active antagonist[54]. Similarly, we found that (R)-phaclofen was the active enantiomer, in agreement with previous studies[55].

The structure of the (R)-baclofen$_{AGO}$-GBR1b$_{VFT}$:GBR2$_{VFT}$ complex was also determined by molecular replacement. The position of GBR2$_{VFT}$ was found using the GBR2$_{VFT}$ structure from the apo complex as the search model. The (R)-baclofen$_{AGO}$-bound GBR1b$_{VFT}$ molecule was located using the individual LB1 and LB2 domains of apo-GBR1b$_{VFT}$ as the search probes. A complete model of the (R)-baclofen$_{AGO}$-GBR1b$_{VFT}$:GBR2$_{VFT}$ complex was constructed through iterative rounds of manual building and refinement. The GABA-bound GBR1b$_{VFT}$:GBR2$_{VFT}$ structure was solved using the refined (R)-baclofen$_{AGO}$-GBR1b$_{VFT}$:GBR2$_{VFT}$ complex structure as the search model. For each complex, the bound agonist was modeled into the residual electron density map obtained in the final rounds of refinement. The (R)-baclofen$_{AGO}$-GBR1b$_{VFT}$:GBR2$_{VFT}$ complex contained the GBR1b$_{VFT}$ residues 50–368 and 377–459; the GABA-GBR1b$_{VFT}$:GBR2$_{VFT}$ complex contained the GBR1b$_{VFT}$ residues 50–84, 92–337, 344–368 and 377–459. Both agonist-bound structures contained the GBR2$_{VFT}$ residues 50–291 and 302–466, and part of the Flag tag at the C-termini of both GBR1b$_{VFT}$ and GBR2$_{VFT}$. Carbohydrate residues were attached to Asn404 of GBR2$_{VFT}$.

Molecular replacement searches were carried out using PHASER[56]. Model building was performed with COOT[57]. Structural refinement was executed using BUSTER[58]. Ramachandran statistics were calculated for each structure using MolProbity[59]. Pairwise structural comparison was performed using LSQMAN[60]. Software installation support was provided by SBGrid[61].

Author Manuscript Author Manuscript Author Manuscript Author Manuscript

Cell surface expression

Full-length human GBR1b and GBR2 were individually cloned into a pcDNA3.1(+) vector (Invitrogen) for expression in human embryonic kidney (HEK293) cells. A Flag tag was inserted after the signal peptide of GBR1b, and an HA tag was placed after the signal peptide of GBR2. Mutants of GBR1b and GBR2 were constructed using the QuikChange mutagenesis system (Stratagene).

HEK293 T/17 cells (ATCC) were co-transfected by Lipofectamine 2000 (Invitrogen) with the GBR1b and GBR2 plasmids. Cells permeabilized with 0.5% Triton X100 were used to determine the total expression levels of GBR1b and GBR2 in transfected cells. Untreated cells were used to determine the cell surface expression level of each subunit. The amount of surface protein detected for each construct was normalized to that found in the total cell lysate.

The cells were blocked with 5% milk, and then incubated with mouse anti-Flag M1 antibody (Sigma) as the primary antibody to measure GBR1b expression. Similarly, mouse anti-HA antibody HA.11 clone 16B12 (Covance) was used to detect GBR2. Donkey anti-mouse IRDye 800-labeled antibody (LiCor) was used as the secondary antibody in both cases. Fluorescent signals were measured with an Odyssey Infrared Imager (LiCor). The results of three independent experiments were used for statistical analysis. All of the mutants reported here were expressed on the cell surface at levels comparable to that of wild-type $GABA_B$ receptor.

Agonist-stimulated [^{35}S]GTPγS binding

HEK293 T/17 cells were transiently transfected with full length GBR1b and GBR2 plasmids. The cells were harvested in 50 mM Hepes, pH 7.4 to obtain the membrane fraction. Membranes were suspended in an assay buffer containing 50 mM Tris pH 7.7, 100 mM NaCl, 12 mM $MgCl_2$, 1.8 mM $CaCl_2$, and 0.2 mM EGTA to approximately 400 μg protein per ml. The membrane homogenates were incubated with increasing concentrations of GABA in the presence of 10 μM GDP. [^{35}S]GTPγS (1,250 Ci/mmol) was then added to a final concentration of 0.5 nM. After incubation at room temperature for 45 minutes, unbound [^{35}S]GTPγS was removed by centrifugation. The amount of bound [^{35}S]GTPγS was measured using a Beckman LS6500 liquid scintillation counter. Nonspecific binding was measured in the presence of 20 μM unlabeled GTPγS. Basal activity was determined in the absence of GABA. The basal activity of the wild-type receptor was used to calculate the percent stimulation of the double cysteine mutant receptor GBR1b-T198C/GBR2-Q206C under non-reducing conditions. The reduced [^{35}S]GTPγS binding activity of the double cysteine mutant (~60% of the wild-type value) could be attributed to the effect of the mutations themselves, since introduction of a single cysteine mutation into either subunit also caused a decrease in agonist response.

To measure [^{35}S]GTPγS binding under reducing conditions, the membrane homogenates were pre-incubated with 1mM dithiothreitol (DTT) before the addition of various concentrations of GABA and 10 μM GDP. The presence of DTT reduced the basal activity of all different combinations of wild-type and cysteine mutant receptors. The percent

Author Manuscript Author Manuscript Author Manuscript Author Manuscript

stimulation of each receptor mutant was calculated based on the wild-type response obtained under the same condition. Data analysis was performed using the non-linear regression algorithms in Prism (GraphPad Software). Data points represent average ± s.e.m. of triplicate measurements.

Radioligand binding assay

HEK293 T/17 cells were transiently transfected with full length GBR1b and GBR2 plasmids. Cell membranes were suspended in an assay buffer containing 20 mM Tris pH 7.4, 118 mM NaCl, 5.6 mM glucose, 1.2 mM KH_2PO_4, 1.2 mM $MgSO_4$, 4.7 mM KCl, and 1.8 mM $CaCl_2$ to approximately 400 μg protein per ml. [^{3}H]CGP54626$_{ANT}$ (25 Ci/mmol) was added to the reaction mixture to final concentrations ranging from 0.5 nM to 20 nM. After incubation at room temperature for 30 minutes, unbound [^{3}H]CGP54626$_{ANT}$ was removed by centrifugation. The amount of bound [^{3}H]CGP54626$_{ANT}$ was measured by liquid scintillation counting. Nonspecific binding was measured in the presence of 10 mM unlabeled GABA. Data analysis was performed using the non-linear regression algorithms in Prism. Data points represent average ± s.e.m. of triplicate measurements.

Disulfide design and western blot analysis

The structure of (R)-baclofen$_{AGO}$-GBR1b$_{VFT}$:GBR2$_{VFT}$ was used for the rational design of disulfide bonds at the LB2-LB2 heterodimer interface. The residue pair, GBR1b-T198 and GBR2-Q206 was identified by the software Disulfide by Design[62] to have the proximity and geometry required for disulfide formation when mutated to cysteines. The T198C and Q206C mutations were engineered into full length GBR1b and GBR2 in pcDNA3.1(+), respectively.

HEK293 T/17 cells were transiently transfected with equal amounts of the full length GBR1b and GBR2 plasmids. Cells were harvested in a buffer containing 20 mM Tris, pH 7.5, 150 mM NaCl, and 1% dodecyl-maltoside. After the insoluble materials were removed by centrifugation, the supernatant was analyzed by 4–15% SDS polyacrylamide gel electrophoresis in the absence and presence of 100 mM DTT. In addition, formation of a disulfide-linked heterodimer between the cysteine mutant pair GBR1b-T198C and GBR2-Q206C was analyzed under two different conditions: in the absence of any ligand, and in the presence of 10 mM GABA. Heterodimer formation of all other samples was analyzed in the presence of 10 mM GABA. The samples were transferred to polyvinylidene fluoride (PVDF) membranes. After blocking with 5% milk, the membranes were incubated with a primary antibody. Mouse anti-Flag M1 antibody (Sigma) was used to detect the GBR1b protein. Mouse anti-HA antibody HA.11 clone 16B12 (Covance) was used to probe GBR2. Both were followed by an alkaline phosphatase (AP)-conjugated anti-mouse secondary antibody. Proteins were visualized by colorimetric method.

Supplementary Material

Refer to Web version on PubMed Central for supplementary material.

Author Manuscript Author Manuscript Author Manuscript Author Manuscript

Acknowledgements

We thank Dr. W.A. Hendrickson and Dr. R. Kass for advice and support, Dr. I. Berger for the gift of pFBDM vector, Drs. K. Rajashankar, K. Perry, S. Banerjee, F. Murphy, I. Kourinov and D. Neau at Advanced Photon Source for help with data collection, Y. Chen for technical assistance, and Dr M. Evelyn for reading the manuscript. This work was supported by the American Heart Association grant SDG0835183N, and the National Institute of Health grant R01GM088454 (both to Q.R.F.). Q.R.F. is an Irma Hirschl Career Scientist, Pew Scholar, McKnight Scholar and Schaefer Scholar.

References

1. Bettler B, Kaupmann K, Mosbacher J, Gassmann M. Molecular structure and physiological functions of GABA(B) receptors. Physiol. Rev. 2004; 84:835–867. [PubMed: 15269338]
2. Bowery NG, et al. International Union of Pharmacology. XXXIII. Mammalian gamma-aminobutyric acid(B) receptors: structure and function. Pharmacol. Rev. 2002; 54:247–264. [PubMed: 12037141]
3. Froestl W. Chemistry and pharmacology of $GABA_B$ receptor ligands. Adv. Pharmacol. 2010; 58:19–62. [PubMed: 20655477]
4. Pin JP, et al. The activation mechanism of class-C G-protein coupled receptors. Biol. Cell. 2004; 96:335–342. [PubMed: 15207901]
5. Romano C, Yang WL, O'Malley KL. Metabotropic glutamate receptor 5 is a disulfide-linked dimer. J. Biol. Chem. 1996; 271:28612–28616. [PubMed: 8910492]
6. Okamoto T, et al. Expression and purification of the extracellular ligand binding region of metabotropic glutamate receptor subtype 1. J. Biol. Chem. 1998; 273:13089–13096. [PubMed: 9582347]
7. Tsuji Y, et al. Cryptic dimer interface and domain organization of the extracellular region of metabotropic glutamate receptor subtype 1. J. Biol. Chem. 2000; 275:28144–28151. [PubMed: 10874032]
8. Bai M, Trivedi S, Brown EM. Dimerization of the extracellular calcium-sensing receptor (CaR) on the cell surface of CaR-transfected HEK293 cells. J. Biol. Chem. 1998; 273:23605–23610. [PubMed: 9722601]
9. Jones KA, et al. GABA(B) receptors function as a heteromeric assembly of the subunits GABA(B)R1 and GABA(B)R2. Nature. 1998; 396:674–679. [PubMed: 9872315]
10. Kaupmann K, et al. GABA(B)-receptor subtypes assemble into functional heteromeric complexes. Nature. 1998; 396:683–687. [PubMed: 9872317]
11. White JH, et al. Heterodimerization is required for the formation of a functional GABA(B) receptor. Nature. 1998; 396:679–682. [PubMed: 9872316]
12. Kuner R, et al. Role of heteromer formation in $GABA_B$ receptor function. Science. 1999; 283:74–77. [PubMed: 9872744]
13. Milligan G. G protein-coupled receptor hetero-dimerization: contribution to pharmacology and function. Br. J. Pharmacol. 2009; 158:5–14. [PubMed: 19309353]
14. Ng GY, et al. Identification of a $GABA_B$ receptor subunit, gb2, required for functional GABAB receptor activity. J. Biol. Chem. 1999; 274:7607–7610. [PubMed: 10075644]
15. Nelson G, et al. Mammalian sweet taste receptors. Cell. 2001; 106:381–390. [PubMed: 11509186]
16. Nelson G, et al. An amino-acid taste receptor. Nature. 2002; 416:199–202. [PubMed: 11894099]
17. Margeta-Mitrovic M, Jan YN, Jan LY. A trafficking checkpoint controls GABA(B) receptor heterodimerization. Neuron. 2000; 27:97–106. [PubMed: 10939334]
18. Pagano A, et al. C-terminal interaction is essential for surface trafficking but not for heteromeric assembly of GABA(b) receptors. J. Neurosci. 2001; 21:1189–1202. [PubMed: 11160389]
19. Kaupmann K, et al. Expression cloning of GABA(B) receptors uncovers similarity to metabotropic glutamate receptors. Nature. 1997; 386:239–246. [PubMed: 9069281]
20. Malitschek B, et al. The N-terminal domain of gamma-aminobutyric Acid(B) receptors is sufficient to specify agonist and antagonist binding. Mol. Pharmacol. 1999; 56:448–454. [PubMed: 10419566]

Author Manuscript Author Manuscript Author Manuscript Author Manuscript

21. Kniazeff J, Galvez T, Labesse G, Pin JP. No ligand binding in the GB2 subunit of the GABA(B) receptor is required for activation and allosteric interaction between the subunits. J. Neurosci. 2002; 22:7352–7361. [PubMed: 12196556]
22. Galvez T, et al. Allosteric interactions between GB1 and GB2 subunits are required for optimal GABA(B) receptor function. EMBO J. 2001; 20:2152–2159. [PubMed: 11331581]
23. Liu J, et al. Molecular determinants involved in the allosteric control of agonist affinity in the $GABA_B$ receptor by the $GABA_B2$ subunit. J. Biol. Chem. 2004; 279:15824–15830. [PubMed: 14736871]
24. Nomura R, Suzuki Y, Kakizuka A, Jingami H. Direct detection of the interaction between recombinant soluble extracellular regions in the heterodimeric metabotropic gamma-aminobutyric acid receptor. J. Biol. Chem. 2008; 283:4665–4673. [PubMed: 18165688]
25. Monnier C, et al. Trans-activation between 7TM domains: implication in heterodimeric GABA(B) receptor activation. EMBO J. 2011; 30:32–42. [PubMed: 21063387]
26. Geng Y, et al. Structure and functional interaction of the extracellular domain of human GABA(B) receptor GBR2. Nat. Neurosci. 2012; 15:970–978. [PubMed: 22660477]
27. Margeta-Mitrovic M, Jan YN, Jan LY. Ligand-induced signal transduction within heterodimeric GABA(B) receptor. Proc. Natl. Acad. Sci. U. S. A. 2001; 98:14643–14648. [PubMed: 11724957]
28. Margeta-Mitrovic M, Jan YN, Jan LY. Function of GB1 and GB2 subunits in G protein coupling of GABA(B) receptors. Proc. Natl. Acad. Sci. U. S. A. 2001; 98:14649–14654. [PubMed: 11724956]
29. Robbins MJ, et al. GABA(B2) is essential for g-protein coupling of the GABA(B) receptor heterodimer. J. Neurosci. 2001; 21:8043–8052. [PubMed: 11588177]
30. Duthey B, et al. A single subunit (GB2) is required for G-protein activation by the heterodimeric GABA(B) receptor. J. Biol. Chem. 2002; 277:3236–3241. [PubMed: 11711539]
31. Havlickova M, et al. The intracellular loops of the GB2 subunit are crucial for G-protein coupling of the heteromeric gamma-aminobutyrate B receptor. Mol. Pharmacol. 2002; 62:343–350. [PubMed: 12130687]
32. Pin JP, et al. Activation mechanism of the heterodimeric GABA(B) receptor. Biochem. Pharmacol. 2004; 68:1565–1572. [PubMed: 15451400]
33. Kunishima N, et al. Structural basis of glutamate recognition by a dimeric metabotropic glutamate receptor. Nature. 2000; 407:971–977. [PubMed: 11069170]
34. Tsuchiya D, Kunishima N, Kamiya N, Jingami H, Morikawa K. Structural views of the ligand-binding cores of a metabotropic glutamate receptor complexed with an antagonist and both glutamate and Gd^{3+} Proc. Natl. Acad. Sci. U. S. A. 2002; 99:2660–2665. [PubMed: 11867751]
35. Muto T, Tsuchiya D, Morikawa K, Jingami H. Structures of the extracellular regions of the group II/III metabotropic glutamate receptors. Proc. Natl. Acad. Sci. U. S. A. 2007; 104:3759–3764. [PubMed: 17360426]
36. van den Akker F, et al. Structure of the dimerized hormone-binding domain of a guanylyl-cyclase-coupled receptor. Nature. 2000; 406:101–104. [PubMed: 10894551]
37. He X, Chow D, Martick MM, Garcia KC. Allosteric activation of a spring-loaded natriuretic peptide receptor dimer by hormone. Science. 2001; 293:1657–1662. [PubMed: 11533490]
38. Jin R, et al. Crystal structure and association behaviour of the GluR2 amino-terminal domain. EMBO J. 2009; 28:1812–1823. [PubMed: 19461580]
39. Karakas E, Simorowski N, Furukawa H. Structure of the zinc-bound amino-terminal domain of the NMDA receptor NR2B subunit. EMBO J. 2009; 28:3910–3920. [PubMed: 19910922]
40. Kumar J, Schuck P, Jin R, Mayer ML. The N-terminal domain of GluR6-subtype glutamate receptor ion channels. Nat. Struct. Mol. Biol. 2009; 16:631–638. [PubMed: 19465914]
41. Sack JS, Saper MA, Quiocho FA. Periplasmic binding protein structure and function. Refined X-ray structures of the leucine/isoleucine/valine-binding protein and its complex with leucine. J. Mol. Biol. 1989; 206:171–191. [PubMed: 2649682]
42. Kniazeff J, et al. Locking the dimeric GABA(B) G-protein-coupled receptor in its active state. J. Neurosci. 2004; 24:370–377. [PubMed: 14724235]

Author Manuscript Author Manuscript Author Manuscript Author Manuscript

43. Rondard P, et al. Functioning of the dimeric GABA(B) receptor extracellular domain revealed by glycan wedge scanning. EMBO J. 2008; 27:1321–1332. [PubMed: 18388862]
44. Galvez T, et al. Mutagenesis and modeling of the $GABA_B$ receptor extracellular domain support a venus flytrap mechanism for ligand binding. J. Biol. Chem. 1999; 274:13362–13369. [PubMed: 10224098]
45. Galvez T, et al. Mapping the agonist-binding site of $GABA_B$ type 1 subunit sheds light on the activation process of $GABA_B$ receptors. J. Biol. Chem. 2000; 275:41166–41174. [PubMed: 10986293]
46. Galvez T, et al. Ca(2+) requirement for high-affinity gamma-aminobutyric acid (GABA) binding at GABA(B) receptors: involvement of serine 269 of the GABA(B)R1 subunit. Mol. Pharmacol. 2000; 57:419–426. [PubMed: 10692480]
47. Kniazeff J, et al. Closed state of both binding domains of homodimeric mGlu receptors is required for full activity. Nat. Struct. Mol. Biol. 2004; 11:706–713. [PubMed: 15235591]
48. Furukawa H, Singh SK, Mancusso R, Gouaux E. Subunit arrangement and function in NMDA receptors. Nature. 2005; 438:185–192. [PubMed: 16281028]
49. Kammerer RA, et al. Heterodimerization of a functional $GABA_B$ receptor is mediated by parallel coiled-coil alpha-helices. Biochemistry. 1999; 38:13263–13269. [PubMed: 10529199]

Methods references

50. Berger I, Fitzgerald DJ, Richmond TJ. Baculovirus expression system for heterologous multiprotein complexes. Nat. Biotechnol. 2004; 22:1583–1587. [PubMed: 15568020]
51. Kabsch W. Xds. Acta Crystallogr. D. Biol. Crystallogr. 2010; 66:125–132. [PubMed: 20124692]
52. Evans P. Scaling and assessment of data quality. Acta Crystallogr. D. Biol. Crystallogr. 2006; 62:72–82. [PubMed: 16369096]
53. Otwinowski Z, Minor W. Processing of X-ray diffraction data collected in oscillation mode. Methods Enzymol. 1997; 276:307–326.
54. Kerr DI, Ong J, Doolette DJ, Schafer K, Prager RH. The (S)-enantiomer of 2-hydroxysaclofen is the active GABAB receptor antagonist in central and peripheral preparations. Eur. J. Pharmacol. 1995; 287:185–189. [PubMed: 8749034]
55. Frydenvang K, et al. GABAB antagonists: resolution, absolute stereochemistry, and pharmacology of (R)- and (S)-phaclofen. Chirality. 1994; 6:583–589. [PubMed: 7986672]
56. McCoy AJ, et al. Phaser crystallographic software. J. Appl. Crystallogr. 2007; 40:658–674. [PubMed: 19461840]
57. Emsley P, Cowtan K. Coot: model-building tools for molecular graphics. Acta Crystallogr. D. Biol. Crystallogr. 2004; 60:2126–2132. [PubMed: 15572765]
58. Roversi P, Blanc E, Vonrhein C, Evans G, Bricogne G. Modelling prior distributions of atoms for macromolecular refinement and completion. Acta Crystallogr. D. Biol. Crystallogr. 2000; 56:1316–1323. [PubMed: 10998628]
59. Chen VB, et al. MolProbity: all-atom structure validation for macromolecular crystallography. Acta Crystallogr. D. Biol. Crystallogr. 2010; 66:12–21. [PubMed: 20057044]
60. Novotny M, Madsen D, Kleywegt GJ. Evaluation of protein fold comparison servers. Proteins. 2004; 54:260–270. [PubMed: 14696188]
61. Morin A, et al. Collaboration gets the most out of software. Elife. 2013; 2:e01456. [PubMed: 24040512]
62. Dombkowski AA. Disulfide by Design: a computational method for the rational design of disulfide bonds in proteins. Bioinformatics. 2003; 19:1852–1853. [PubMed: 14512360]

Author Manuscript Author Manuscript Author Manuscript Author Manuscript

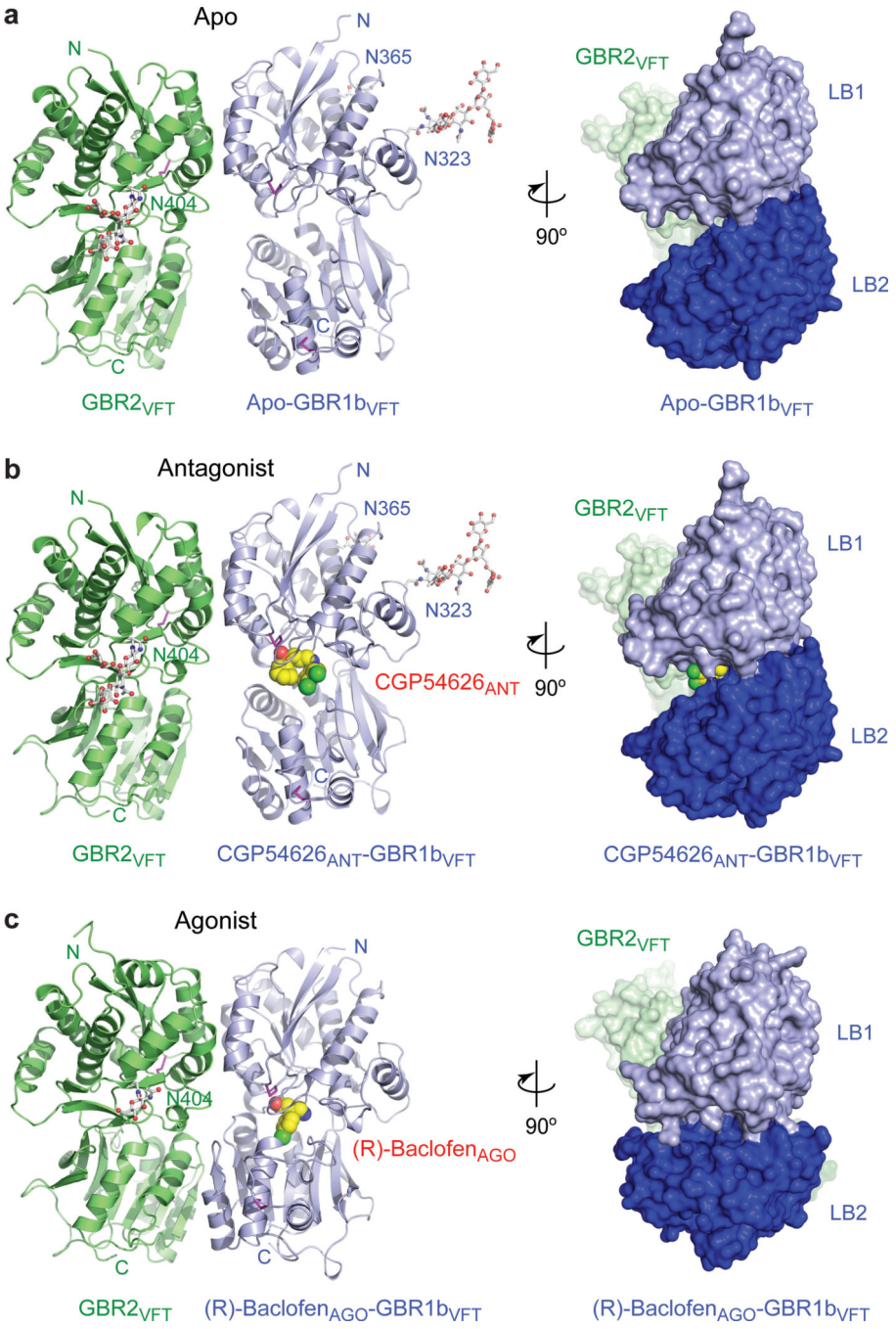

Figure 1. Crystal structures of the $GBR1b_{VFT}$:$GBR2_{VFT}$ complex

a, Apo structure. **b,** Antagonist $CGP54626_{ANT}$-bound structure. **c,** Agonist (R)-$baclofen_{AGO}$-bound structure. Each complex is shown in two views related by a 90°-rotation about the vertical axis. Front view (left panel) is shown as a ribbon diagram; side view (right panel) is presented as a molecular surface. $GBR1b_{VFT}$ and $GBR2_{VFT}$ are colored blue and green, respectively. The observed carbohydrates are shown as ball-and-stick models in gray. Disulfide bridges are in magenta. The ligands are displayed as space-filling models.

Author Manuscript Author Manuscript Author Manuscript Author Manuscript

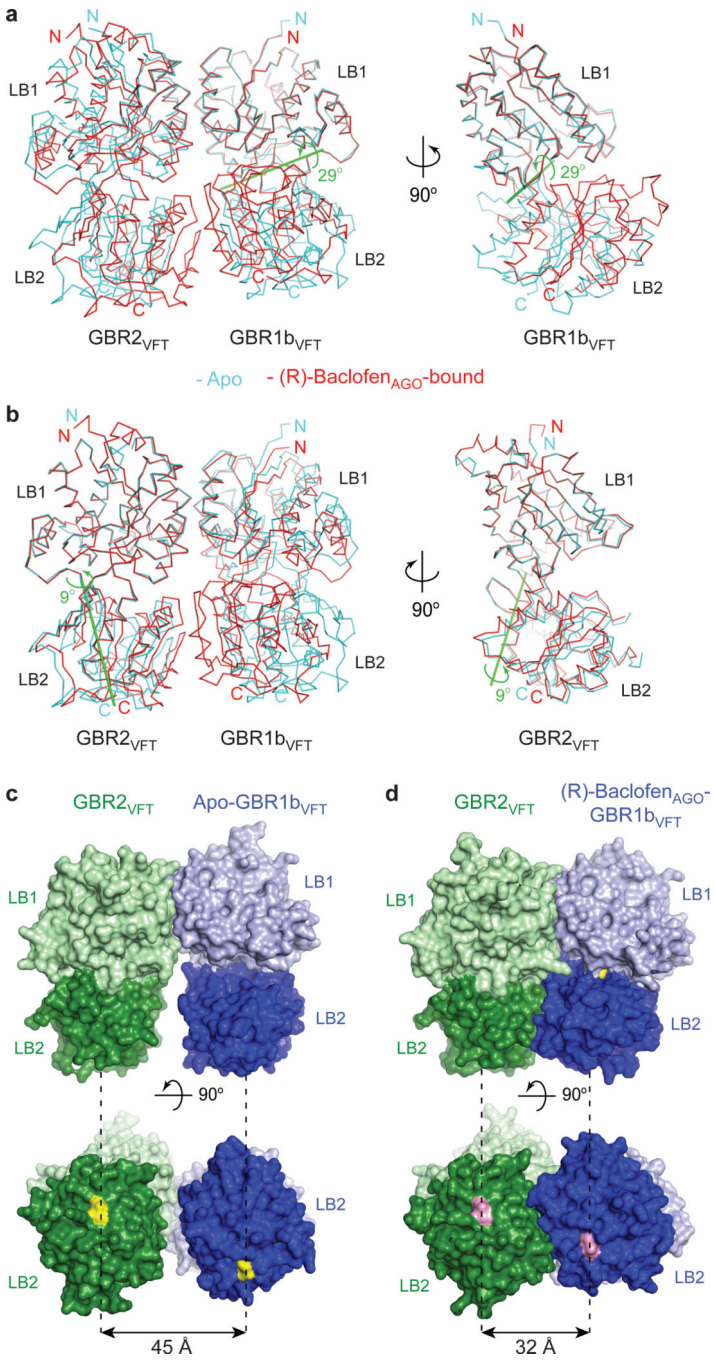

Figure 2. Agonist-induced conformational changes

a, b, Superposition of apo (cyan) and (R)-baclofen$_{AGO}$-bound (red) complexes based on the LB1 domain of GBR1b$_{VFT}$ **(a)**, or GBR2$_{VFT}$ **(b)**. Side view is shown on the right for the superimposed GBR1b$_{VFT}$ **(a)** and GBR2$_{VFT}$ **(b)** subunits. Green line is the axis of rotation that relates the LB2 domain of GBR1b$_{VFT}$ (rotation χ = 29°, screw translation τ_χ = 0.2 Å) **(a)** or GBR2$_{VFT}$ (rotation χ = 9°, screw translation τ_χ = 0.1 Å) **(b)** from the apo and agonist-bound structures.

Author Manuscript Author Manuscript Author Manuscript Author Manuscript

c, d, Surface representation of apo **(c)** and (R)-baclofen$_{AGO}$-bound **(d)** GBR1b$_{VFT}$:GBR2$_{VFT}$ in front view (top), and bottom view (bottom). Distances between C-termini of the two subunits (yellow in apo structure; pink in (R)-baclofen$_{AGO}$-bound structure) are marked by dashed lines.

Author Manuscript Author Manuscript Author Manuscript Author Manuscript

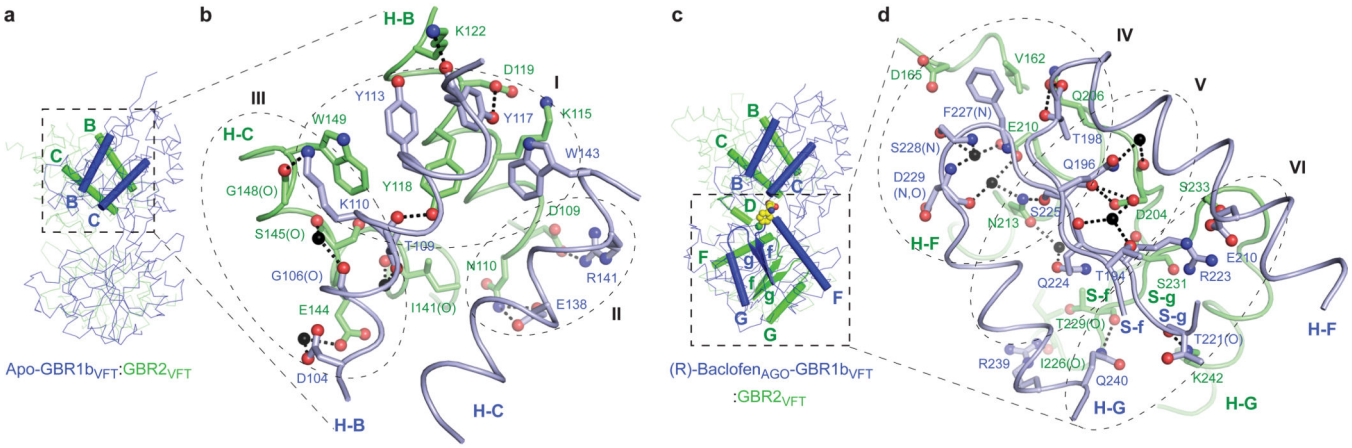

Figure 3. Heterodimer interface

a, Structure of apo-GBR1b$_{VFT}$:GBR2$_{VFT}$ with the elements involved in heterodimer formation highlighted by ribbons (LB1-LB1: B and C helices). **b,** Specific contacts at the LB1-LB1 heterodimer interface of apo-GBR1b$_{VFT}$:GBR2$_{VFT}$. The interface area is divided into three regions I, II, and III. Dashed lines indicate hydrogen bonds.

c, Structure of (R)-baclofen$_{AGO}$-GBR1b$_{VFT}$:GBR2$_{VFT}$ showing the elements involved in heterodimer formation (LB1-LB1: B and C helices; LB2-LB2: F and G helices, f and g strands, and connecting loops). **d,** Specific contacts at the LB2-LB2 heterodimer interface of (R)-baclofen$_{AGO}$-GBR1b$_{VFT}$:GBR2$_{VFT}$. The interface area is divided into three regions IV, V, and VI. Dashed lines indicate hydrogen bonds.

Author Manuscript Author Manuscript Author Manuscript Author Manuscript

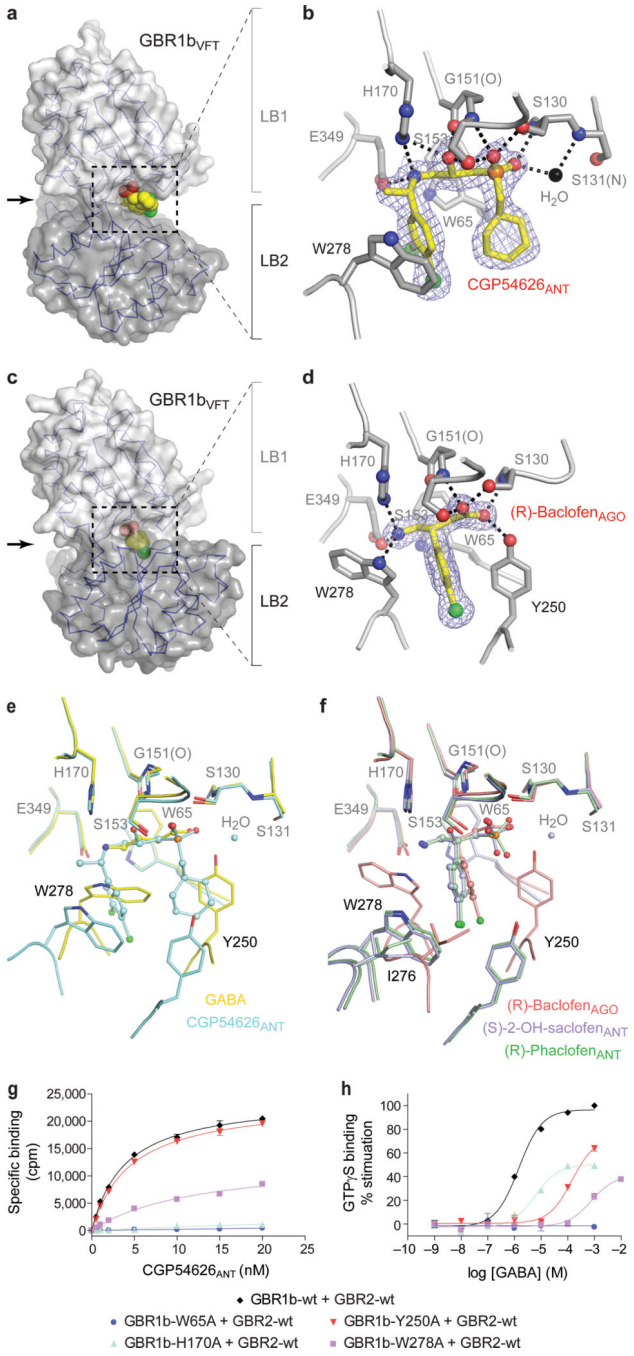

Figure 4. Ligand recognition by GBR1b$_{VFT}$

a, c, Molecular surface of GBR1b$_{VFT}$ bound to antagonist CGP54626$_{ANT}$ **(a)** or agonist (R)-baclofen$_{AGO}$ **(c)**. Ligand is displayed as a space-filling model.

b, d, Specific contacts between GBR1b$_{VFT}$ (gray) and CGP54626$_{ANT}$ (yellow) **(b)** or (R)-baclofen$_{AGO}$ **(d)**, viewed in the direction of the arrow in **a** or **c**. Mesh represents the final 2Fo-Fc electron density map contoured at 1σ. Hydrogen bonds are represented by black dashed lines.

Author Manuscript Author Manuscript Author Manuscript Author Manuscript

e, Comparison of the binding sites of agonist GABA and antagonist $CGP54626_{ANT}$. **f,** Comparison of the binding sites of agonist (R)-$baclofen_{AGO}$ and two related antagonists (S)-2-OH-$saclofen_{ANT}$ and (R)-$phaclofen_{ANT}$.

g, h, Dose-dependent [^{3}H]$CGP54626_{ANT}$ binding **(g)** and GABA-stimulated [^{35}S]GTPγS binding **(h)** in membranes from cells expressing wild type $GABA_B$ receptor (GBR1b-wt + GBR2-wt) or the combination of GBR2-wt and various GBR1b mutants.

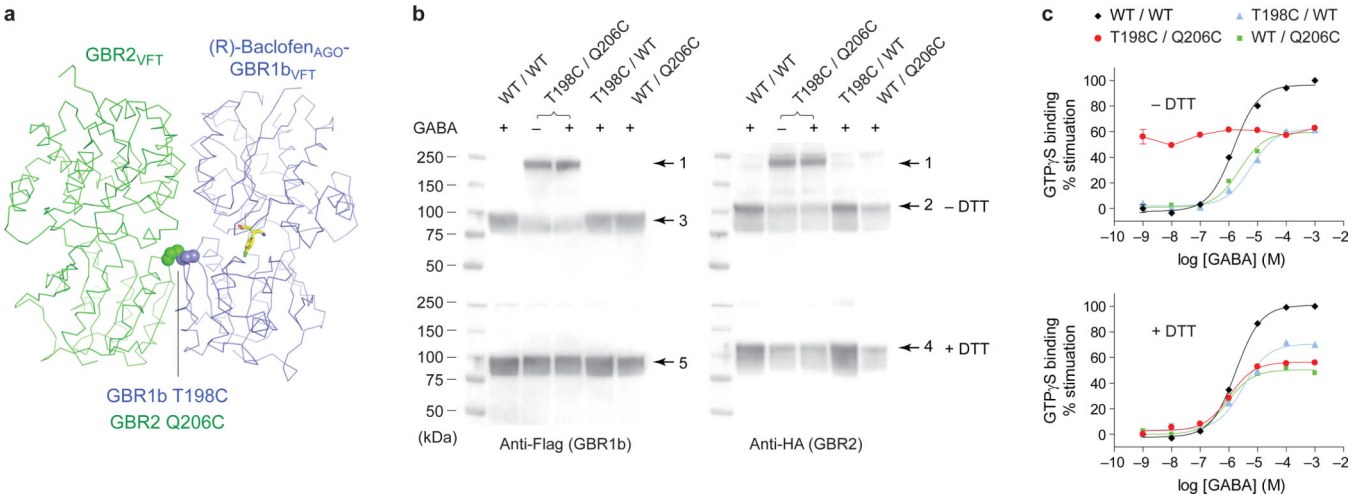

Figure 5. Constitutive activity of disulfide-tethered GBR1b:GBR2 heterodimer

a, Position of cysteine mutations (spheres) at the LB2-LB2 heterodimer interface of (R)-baclofen$_{AGO}$-GBR1b$_{VFT}$:GBR2$_{VFT}$.

b, Western blot analysis of membranes from cells expressing different combinations of wild-type (WT) and mutant GABA$_B$ receptor subunits (GBR1b-T198C, abbreviated as T198C; GBR2-Q206C, abbreviated as Q206C). The samples were assayed in the presence of 10 mM GABA under reducing (+DTT) and non-reducing (−DTT) conditions. The double cysteine mutant (T198C / Q206C) was also analyzed in the absence of ligand. GBR1b and GBR2 were detected by anti-Flag and anti-HA antibodies, respectively. Arrow 1, GBR1b-GBR2 heterodimer; arrow 2 and 4, GBR2 monomer; arrow 3 and 5, GBR1b monomer.

c, GABA-stimulated dose-dependent [^{35}S]GTPγS binding in membranes from cells expressing wild-type or various cysteine mutant receptors in the presence and absence of DTT.

Author Manuscript Author Manuscript Author Manuscript Author Manuscript